



## Assessment of a hollow cylindrical Ti–TiO<sub>2</sub>/IrO<sub>2</sub>/RuO<sub>2</sub> mesh electrode for effective treatment of hospital wastewater using a portable electrochemical reactor

Vinoth kumar Palur Manoharan<sup>a</sup>, Perumal Dhandapani<sup>b,c</sup>, Madhan Kumar Pichandi<sup>d</sup>, Aruliah Rajasekar<sup>e</sup>, Punniyakotti Parthipan<sup>f</sup>, Rajyoganandh Subramanian Vijayaraman<sup>a</sup>, S.M. Prasad<sup>g</sup>, Sudharsan Kasirajan<sup>a,\*</sup>

<sup>a</sup> Department of Microbiology, Vels Institute of Science and Technology & Advanced Studies (VISTAS) Pallavaram, Chennai, Tamil Nadu, 600117, India

<sup>b</sup> Centre for Material Science, Easwari Engineering College, Chennai, Tamil Nadu, 600089, India

<sup>c</sup> Centre for Research, SRM TRP Engineering College, Tiruchirappalli, Tamil Nadu, 621105, India

<sup>d</sup> Nano & Energy BioScience Laboratory, Department of Biotechnology, Thiruvalluvar University, Serkkadu, Vellore, Tamil Nadu, 632115, India

<sup>e</sup> Environmental Molecular Microbiology Research Laboratory, Department of Biotechnology, Thiruvalluvar University, Serkkadu, Vellore, Tamil Nadu, 632115, India

<sup>f</sup> Department of Biotechnology, Faculty of Science and Humanities, SRM Institute of Science and Technology, Kattankulathur, Chengalpattu, Tamil Nadu, 603203, India

<sup>g</sup> Department of Nutrition and Dietetics, Sadakathullah Appa College, Rahmath Nagar, Tirunelveli, Tamil Nadu, 627011, India

### ARTICLE INFO

#### Keywords:

Hospital wastewater  
Electrochemical reactor  
Hollow cylindrical electrode  
Electrochemical oxidation process  
Degradation mechanisms and Toxicity assessments

### ABSTRACT

Hospital wastewater (HWW) comprises a complex matrix of organic and inorganic contaminants, pathogenic microorganisms, and heavy metals that pose significant environmental and public health concerns. This study investigates the performance of a compact and field-deployable electrochemical oxidation (EO) reactor comprising a Ti–TiO<sub>2</sub>/IrO<sub>2</sub>/RuO<sub>2</sub> hollow cylinder anode in raw HWW was investigated in this work. A careful analysis of the physicochemical parameters of HWW showed high concentrations of total dissolved solids (4,567 mg L<sup>-1</sup>), total suspended solids (2,836 mg L<sup>-1</sup>), COD (3,108 mg L<sup>-1</sup>), and BOD (1,230 mg L<sup>-1</sup>). The EO process was performed at current densities 5.8, 10.4 and 15.5 mA/cm<sup>2</sup> and maximum COD removal (92 %) at 15.5 mA/cm<sup>2</sup> after 10h of treatment. The compact anode possessed a crack-propagated surface morphology that is beneficial for Cl<sub>2</sub> evolution reaction, and flower-like scale deposits with mainly Ca and Mg phases revealed by XRD were observed on the cathode, and verified by HR-SEM and EDX. The EO process effectively eliminated both fecal and total coliforms within 60 min and significantly decreased the levels of heavy metals (Fe: 945 → 450, Cu: 732 → 345, Zn: 650 → 140, Mn: 68 → 15 and Pb: 20 → 5.0 ppm). FT-IR and GC-MS studies showed significant degradation of organic compounds, which resulted in the reduction of toxic substances and the production of less harmful products. The treatment is enhanced by in-situ generated active chlorine species (Cl<sub>2</sub>, HOCl and OCl<sup>-</sup>), that oxidize and mineralize organic-matter. These findings confirm that the EO process has the potential for effective treatment of HWW, resulting in environmental-safe reuse of treated HWW for irrigation use and reduced the environmental footprint of hospitals.

### 1. Introduction

Hospital wastewater HWW originates from various departments within healthcare facilities, including surgical units, dialysis centres, oncology wards, orthopaedic, pediatric units, diagnostic laboratories, and infectious disease wards, excluding washroom areas [1]. This effluent exhibits a complex composition attributable to a diverse array of contaminants, like pharmaceutical residues, various organic

disinfectants, chemical reagents tested in diagnostic procedures, human metabolites, and infectious biological materials [1,2]. Moreover, the presence of diverse aerobic and anaerobic pathogenic microorganisms further complicates the characteristics of HWW [2]. The prevalence of synthetic pharmaceuticals and chemical reagents from healthcare facilities significantly elevates the organic pollutant load in HWW, thereby promoting the proliferation of antibiotic-resistant microorganisms [2]. Conventional sewage treatment processes generally prove insufficient in

\* Corresponding author.

E-mail address: [sudharsan.micro22@gmail.com](mailto:sudharsan.micro22@gmail.com) (S. Kasirajan).

<https://doi.org/10.1016/j.jics.2025.101985>

Received 3 April 2025; Received in revised form 9 July 2025; Accepted 26 July 2025

Available online 29 July 2025

0019-4522/© 2025 Indian Chemical Society. Published by Elsevier B.V. All rights are reserved, including those for text and data mining, AI training, and similar technologies.

effectively managing this highly contaminated effluent, often leading to its discharge into aquatic and terrestrial ecosystems [3]. This scenario exacerbates the spread of pollutants and pathogens, posing significant risks to both public health and environmental stability. Consequently, HWW has emerged as a critical reason for water pollution, highlighting the imperative need for the development and implementation of effective mitigation strategies.

The treatment of pharmaceutical wastewater and HWW has been effectively tackled through a combination of physical adsorption, biodegradation, and advanced oxidation processes (AOPs) [4–10]. However, each of these methodologies has distinct advantages and drawbacks [10]. Physical treatment methods, which encompass adsorption and filtration, demonstrate high efficiency in the rapid removal of both organic and inorganic contaminants via specialized adsorbent materials [4–7]. These techniques often generate secondary pollutants and require further degradation processes, in addition to the periodic replacement of adsorbent materials [10]. Biological treatment strategies involve the demineralization of organic pollutants using a diverse array of aerobic and anaerobic microorganisms that employ various metabolic enzymes [5]. Notably, these biological processes require extended operating times to achieve significant degradation of organic compounds [5]. In the event of these challenges, AOPs were evaluated for their ability to achieve high removal efficiencies within reduced operational time [10–12]. This is accomplished through the generation of reactive oxygen species (ROS) via various catalytic activation methods, electrochemical reactions, and photo-induced mechanisms [11,29]. Among the AOPs, electrochemical oxidation processes (EOs) have shown considerable effectiveness in degrading pollutants and eradicating pathogens in HWW by generating active chlorine species ( $\text{Cl}_2$ ,  $\text{HClO}$ ,  $\text{OCl}^-$ ) at the anode surface [13]. Selecting appropriate anode materials, using optimized current density, and designing efficient electrochemical reactors are critical factors in enhancing the efficiency of EO processes while reducing operational costs [13–15]. Previous research has demonstrated that the selection of anode materials ( $\text{SnO}_2$ ,  $\text{PbO}_2$ ,  $\text{Ta}_2\text{O}_5$ ,  $\text{RuO}_2$ ,  $\text{IrO}_2$ ,  $\text{Ti}_4\text{O}_7$ , and their complexes) can substantially influence chemical oxygen demand (COD) removal under optimal EO operational conditions [15–17]. Specifically, titanium (Ti) supports coated with metal oxides have been proven to significantly enhance electrocatalytic activity for chlorine and oxygen evolution reactions, which are extensively utilized within the chlor-alkali sector due to their greater catalytic properties and durability [18]. Recent studies have highlighted the use of  $\text{Ti-TiO}_2/\text{IrO}_2/\text{RuO}_2$  electrodes and their influence on COD removal efficiency in various industrial wastewater treatment processes [19–21]. The substantial concentration of chloride ions ( $\text{Cl}^-$ ) present in the effluent facilitates the electrochemical generation of active chlorine species via anodic oxidation. This phenomenon effectively enhances the degradation of various organic contaminants through an indirect oxidation pathway [20]. The efficiency of COD removal in wastewater treatment at pilot scale up is contingent upon several critical parameters, including current density, electrode configuration, concentration of electroactive species, and prevailing hydrodynamic conditions [16–20]. In particular, current density is vital for the optimization and scalability of EO processes [21]. The preference for continuous-flow reactors over batch systems is largely due to the enhanced mass and charge transfer of electroactive species and pollutants in the wastewater matrix [19–22]. Consequently, conventional viable wastewater treatment facilities utilize continuous-flow reactor configurations [13,15,22]. This highlights the demand for innovative design and fabrication methodologies for portable electrochemical reactors such advancements are imperative for effectively targeting contaminants in both industrial and domestic wastewater treatment applications.

This study explores the optimization of the EO process for treating HWW, and aims to achieve substantial reductions in COD while effectively eliminating pathogenic bacteria. A portable electrochemical reactor has been developed, featuring a hollow cylindrical  $\text{Ti-TiO}_2/$

$\text{IrO}_2/\text{RuO}_2$  mesh electrode as the anode and a Ti mesh cathode. A key focus of using this reactor is to investigate the effect of current density on COD removal performance. In addition, the study assesses the generation of active chlorine species during the EO process at various current densities. The level of microbial inactivation, particularly fecal coliforms and total coliforms in wastewater, was evaluated using the Most Probable Number (MPN) method and total viable bacterial count method. The degradation products resulting from EO treatment were characterized using Fourier-transform infrared spectroscopy (FT-IR) and gas chromatography-mass spectrometry (GC-MS). The exploration also investigates the crystal phase characteristics and morphology of hardness-causing species that are electrodeposited on the cathode surface. The heavy metal ion removal efficiency is determined through atomic absorption spectroscopy (AAS). Furthermore, the recycling efficacy of the EO process and the stability of the electrode material are evaluated using X-ray diffraction (XRD). In addition, the raw HWW and its intermediates were evaluated for acute and chronic toxicity to aquatic organisms utilizing the ECOSAR tool (Ecological Structure Activity Relationships). This research provide a novel, compact, new miniaturized and readily adaptable to field use type of EO system using  $\text{Ti-TiO}_2/\text{IrO}_2/\text{RuO}_2$  mesh hollow cylinder shape anode for cables raw HWW treatment. The spherical electrodes as well are definitely better than the flat, but the increasing of the surface, the mass transfer and the efficiency of the chlorine evolution are better using the hollow cylindrical geometry. Maximum degradation of COD was achieved (92 % maximum), along with microbial inactivation and decrease in heavy metals at the optimum current densities. Absolutely necessary, for the first time in the literature are the coupling of these physicochemical, microbiological and spectroscopic (FT-IR and GC-MS) with showed ecotoxicological (ECOSAR) evaluations that is needed to fully evaluate the performance of treatment and including assess the environmental safety. The technology combines state-of-the-art materials science with a real-world HWW remediation, and provides a possible scaleable and power-efficient alternative to existing EO. The focus on employing a hollow cylindrical  $\text{Ti-TiO}_2/\text{IrO}_2/\text{RuO}_2$  mesh electrode for HWW treatment, along with scalability considerations, holds significant potential for advancing the practical implementation of EO technologies in HWW management.

## 2. Materials and methods

### 2.1. Chemicals

Potassium Di Chromate Crystals ( $\text{K}_2\text{Cr}_2\text{O}_7$ ), Mercuric Sulphate Crystals ( $\text{HgSO}_4$ ), Concentrated Sulphuric acid ( $\text{H}_2\text{SO}_4$ ), Silver Sulphate Crystals ( $\text{Ag}_2\text{SO}_4$ ), Ferric Ammonium Sulphate Crystals ( $(\text{NH}_4)_3\text{Fe}(\text{SO}_4)_2 \cdot 12\text{H}_2\text{O}$ ), Orthophosphoric acid ( $\text{H}_3\text{PO}_4$ ), Sodium fluoride, Diphenyl amine indicator ( $(\text{C}_6\text{H}_5)_2\text{NH}$ ), Ferrioin indicator ( $[\text{Fe}(\text{C}_{12}\text{H}_8\text{N}_2)_3]\text{SO}_4$ ), Potassium Iodide Ammonium Molybdate ( $(\text{NH}_4)_6\text{Mo}_7\text{O}_{24} \cdot 4\text{H}_2\text{O}$ ), Methanol solvent ( $\text{CH}_3\text{OH}$ ), Nitric acid ( $\text{HNO}_3$ ), Hydrochloric acid ( $\text{HCl}$ ), Nutrient Agar (NA) and deionised Milli-Q-water were purchased from Hi-Media (Mumbai, India).

### 2.2. Collection of hospital wastewater

HWW was collected from a primary urban center in Vellore of Tamil Nadu, India. A total of 25 L of stagnant water, which had been held for approximately 20 days, was collected in a high-density polyethylene Jerrican. The samples were transported to the Microbiology and Molecular Research (MMR) Laboratory at Vels University. The collected volume was stored refrigerated at temperatures ranging from 4 °C to 8 °C for further analytical procedures.

### 2.3. Experimental set-up and the EO process

The experimental apparatus is detailed in supporting information

(Fig. S1). It consists of an EO reactor constructed from 8-mm thick glass. The base reactor was designed as a cuboid with dimensions of  $6 \times 6 \times 11$  cm (Length x Width x Height), incorporating a central inlet with a 0.5 cm diameter hole. The chamber's base was further extended to dimensions of  $10 \times 10 \times 4$  cm (Length x Width x Height), with a 0.5 cm diameter outlet located at the bottom right side. The reactor had a total volume of 600 ml, and wastewater flow was regulated using a portable mini water pump. The anode and cathode materials were procured from Ti Fab Engineering in Chennai, Tamil Nadu. The anode is composed of a titanium substrate coated with a composite of triple metal oxides (Ti-TiO<sub>2</sub>/IrO<sub>2</sub>/RuO<sub>2</sub>), fabricated into a hollow cylindrical electrode with a diamond-pattern mesh design measuring 3.5 cm in diameter and 8.5 cm in height. The cathode, crafted from pure Ti, featured a design analogous to the anode but with an increased diameter of 4.5 cm and a height of 8.5 cm. Both electrodes were connected to a DC power supply to facilitate the continuous operation of the reactor. Prior to initiating the EO process, the wastewater was thoroughly circulated through the reactor using the pump for 30 min to ensure adequate mixing. Each EO experiment was performed over 10 h at current densities of 5.8, 10.4, and 15.5 mA/cm<sup>2</sup>. All tests were conducted under ambient temperature conditions. Wastewater samples were collected at regular intervals for Chemical Oxygen Demand (COD). In addition, key parameters, including total hardness, total Kjeldahl nitrogen (N-TKN), ammonia (NH<sub>3</sub>), nitrate (NO<sub>3</sub>), nitrite (NO<sub>2</sub>), and Biological Oxygen demand (BOD), were assessed at the end of each experiment.

#### 2.4. Analytical procedure

The pH of the HWW samples was measured using a portable pH meter (Wellon). Conductivity measurements were obtained using a portable EUTECH conductivity meter (Eutech CON 450). Turbidity, total dissolved solids (TDS), and total suspended solids (TSS) were assessed using standard protocols established by the American Public Health Association (APHA, 2017) [23]. Chloride (Cl<sup>-</sup>) and sulphate (SO<sub>4</sub><sup>-</sup>) ions were analyzed using volumetric methods (Mohr's method) and gravimetric methods. Total hardness, along with calcium (Ca<sup>2+</sup>) and magnesium ions (Mg<sup>2+</sup>) concentrations, was determined through titration and AAS techniques. N-TKN, NH<sub>3</sub>, NO<sub>3</sub>, and NO<sub>2</sub> were measured following standard methods (APHA, 2017) [23]. BOD for both raw HWW and EO-treated samples was estimated using BOD bottles incubated at 25 °C for 5 days. Bacteriological parameters, including fecal coliforms (CFU/100 ml) and total coliforms (CFU/100 ml), were analyzed using the Most Probable Number (MPN) technique [24]. Active chlorine produced during the EO treatment was quantified using the iodometry method [22]. COD for both the raw HWW and EO-treated samples was determined by digesting the samples with potassium dichromate, followed by quantification with a spectrophotometer (Spectroquant®, Merck, Germany).

The raw HWW and EO-treated samples were subjected to lyophilization to obtain dried material. The dried samples were then incorporated into KBr pellets for FT-IR analysis using a PerkinElmer Inc [25,26]. Subsequently, the dried samples were dispersed in methanol and filtered through a polytetrafluoroethylene (PTFE) syringe filter (0.22 μm). The identification of organic and intermediate compounds present in both the raw HWW and EO-treated samples was accomplished through GC-MS analysis (an Agilent 6890 N gas chromatograph coupled with a HP 5973 mass spectrometer detector) [27]. The elemental analysis of raw HWW was performed by X-ray fluorescence (XRF) with a Horiba instrument. The morphological characteristics of the anode and cathode materials were assessed by High Resolution-Scanning Electron Microscopy (HR-SEM) coupled with Energy-dispersive X-ray spectroscopy (EDX) using a Thermo Scientific Apreo S system. To analyze the crystal phase of the recovered precipitate from the Ti electrode surface after the EO process was performed using XRD (Bruker D8-ADVANCE unit) [28]. Additionally, Atomic Absorption Spectroscopy (AAS) was used to quantify heavy metal ions in both the raw HWW and EO-treated

samples, following acid digestion for sample preparation [21]. The electrochemical energy expenditure for the EO treatment of HWW was determined using Equation (1) [22].

$$\text{Energy consumption kWh m}^{-3} = \frac{1}{V_s} \int_0^t V I dt \quad (1)$$

V represents the applied voltage (V), A denotes the applied current (A), t indicates the treatment duration (h), and V<sub>s</sub> is the volume of the solution (L).

#### 2.5. Theoretical toxicity assessment

The raw HWW and its intermediates generated through the EO process were assessed for their toxicity to aquatic organisms using the ECOSAR tool 2.2 [29]. Both acute and chronic toxicity (ChV) values for fish, Daphnia, and green algae were evaluated and correlated with the relevant classifications established by the Globally Harmonized System of Classification and Labelling of Chemicals (GHS).

#### 2.6. Statistical analysis

Every experiment was conducted in triplicate (n = 3), and the mean ± standard deviation (SD) was used to display the data. Groups were compared using Dunnett's test after one-way analysis of variance (ANOVA) (GraphPad Prism software). At p < 0.05, statistical significance was established.

### 3. Results and discussion

#### 3.1. Physicochemical characteristics of HWW

(Table 1) presents a comparative analysis of the physicochemical properties of raw HWW and its EO treatment. The wastewater exhibited brown coloration with a slight black tint and an odour, with a recorded pH of  $7.42 \pm 0.2$ . The turbidity was measured at 13 NTUs. Total dissolved solids (TDS) and total suspended solids (TSS) were quantified at  $4567 \pm 26.0$  mg L<sup>-1</sup> and  $2836 \pm 21.0$  mg L<sup>-1</sup>, respectively, indicating a significant presence of organic matter and metal complexes. The HWW sample was characterized by a conductivity of  $1691 \pm 5.0$  μS/cm, consistent with the dissolution of mineral ions. Moreover, concentrations of total hardness, total alkalinity, calcium (Ca), magnesium (Mg), and total phosphate (PO<sub>4</sub>) were determined to be  $1400 \pm 12.5$ ,  $680 \pm 11.5$ ,  $480 \pm 3.0$ ,  $160 \pm 5.0$ , and  $0.5 \pm 0.0$  mg L<sup>-1</sup>, respectively, suggesting a propensity for scale formation within the wastewater. Chloride (Cl<sup>-</sup>) and sulphate (SO<sub>4</sub><sup>-</sup>) ions were present at concentrations of  $1800 \pm 16.0$  and  $980 \pm 13.0$  mg L<sup>-1</sup>, respectively. The presence of Cl<sup>-</sup> ions is notable due to their role in promoting the generation of indirect hypochlorite at the anode surface (Ti-TiO<sub>2</sub>/IrO<sub>2</sub>/RuO<sub>2</sub>) during the EO process, which facilitates organic degradation [18–20]. The analysis also revealed total Kjeldahl nitrogen, NH<sub>3</sub>, NO<sub>3</sub>, and NO<sub>2</sub> levels of  $140 \pm 2.0$ ,  $3.00 \pm 0.1$ ,  $28 \pm 2.5$ , and  $0.14 \pm 0.0$  mg L<sup>-1</sup>, respectively. COD and BOD were measured at  $3108 \pm 18.0$  and  $1230 \pm 9.0$  mg L<sup>-1</sup>, indicating a substantial organic load in HWW. Faecal coliforms and total coliforms counts were presented at 50 and 30 CFU/100 ml, respectively. The supplementary information (Fig. S2) comprehensively details the XRF analysis of the raw HWW. The results indicate a predominant calcium (Ca) concentration of 80.40 %, accompanied by significant levels of iron (Fe) at 7.43 %, phosphorus (P) at 5.35 %, and sulfur (S) at 3.83 %. Additionally, trace elements are present in the following concentrations: zinc (Zn) at 0.79 %, manganese (Mn) at 0.44 %, titanium (Ti) at 0.40 %, lead (Pb) at 0.29 %, copper (Cu) at 0.27 %, and chromium (Cr) at 0.07 %. The physicochemical analysis demonstrates elevated COD, BOD, and heavy metal levels, alongside the presence of diverse coliform bacterial species in the HWW. These findings highlight the persistent necessity for the advancement of effective electrochemical techniques designed to

**Table 1**

Comparative analysis of the characteristics of raw HWW and after EO treatment, by the specifications outlined in IS 10500: 2012 and the World Health Organization (WHO) guidelines for irrigation water quality.

S.No	Parameters	Raw HWW	EO treatment	Specification as per IS 10500: 2012		WHO
				Acceptable limit	Permissible limit	
1	Appearance	Sly-Turbid	–	–	–	–
2	Colour (Hazen)	Brownish	White	Agreeable	Agreeable	–
3	Odour	Some odour	–	–	–	–
4	pH	7.42 ± 0.20	7.0 ± 0.20	6.5–8.5	6.5–8.5	5.5–9.0
5	Turbidity (NTU)	13 ± 0.10	4.5 ± 0.10	1	5	–
6	Total dissolved solids (mg L <sup>-1</sup> )	4567 ± 26.0	760 ± 11.4	500	2000	1500
7	Total suspended solids (mg L <sup>-1</sup> )	2836 ± 21.0	380 ± 8.2	–	–	–
8	Conductivity (µS/cm)	1691 ± 5.0	1425 ± 9.8	–	–	–
9	Total Hardness (mg L <sup>-1</sup> )	1400 ± 12.5	280 ± 4.8	200	600	–
10	Calcium (mg L <sup>-1</sup> )	480 ± 3.0	72 ± 2.5	75	200	–
11	Magnesium (mg L <sup>-1</sup> )	160 ± 5.0	38 ± 2.2	30	100	–
12	Total Alkalinity (mg L <sup>-1</sup> )	680 ± 11.5	118 ± 6.4	200	600	–
13	Total Phosphate as PO <sub>4</sub> (mg L <sup>-1</sup> )	0.5 ± 0.0	0.2 ± 0.0	–	–	0.1
14	Chloride (mg L <sup>-1</sup> )	1800 ± 16.0	860 ± 15.4	250	1000	250
15	Sulphate (mg L <sup>-1</sup> )	980 ± 13.0	520 ± 9.8	200	400	200
16	Total kjedhal nitrogen (mg L <sup>-1</sup> )	140 ± 2.0	0.00	–	–	–
17	Ammonia (mg L <sup>-1</sup> )	3.00 ± 0.1	0.4 ± 0.0	0.5	0.5	2
18	Nitrate (mg L <sup>-1</sup> )	28 ± 2.5	4.5 ± 0.1	45	45	45
19	Nitrites (mg L <sup>-1</sup> )	0.14 ± 0.0	0.06 ± 0.0	–	–	–
20	Oil and grease (mg L <sup>-1</sup> )	50 ± 4.0	0.00	–	–	–
21	Chemical oxygen demand (mg L <sup>-1</sup> )	3108 ± 18.0	220 ± 8.8	250	500	500
22	Biological oxygen demand (at 27 °C for 3 Days) (mg L <sup>-1</sup> )	1230 ± 9.0	180 ± 4.6	–	–	200
23	Fecal Coliforms (CFU/100 ml)	50	0.00	0	0	–
24	Total Coliforms (CFU/100 ml)	30	0.00	0	0	–

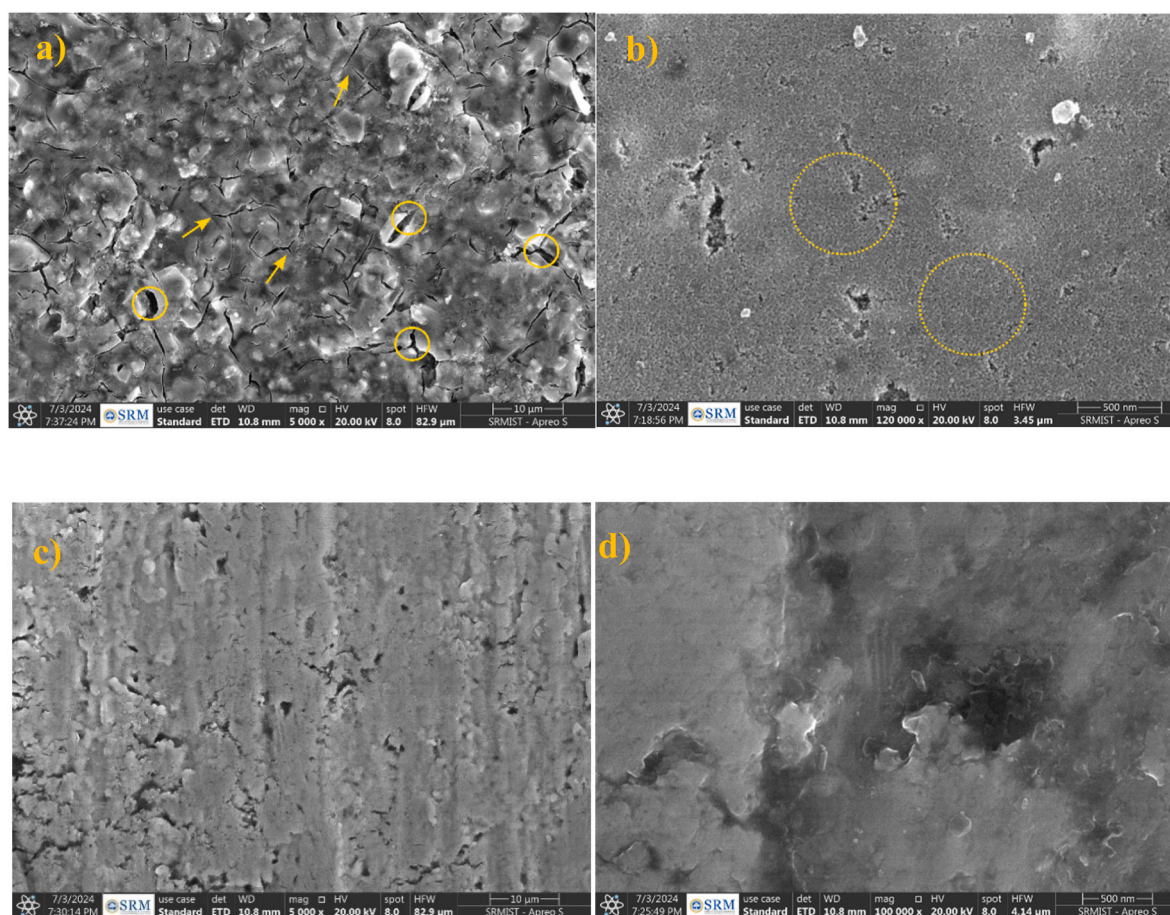


**Fig. 1.** (a & b) HR-SEM images of the pristine Ti-TiO<sub>2</sub>/IrO<sub>2</sub>/RuO<sub>2</sub>, and (c & d) Ti electrode.

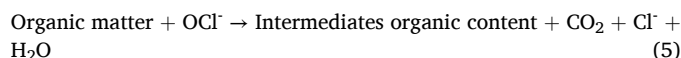
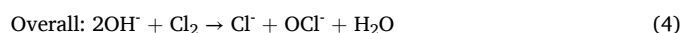
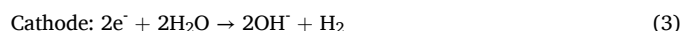
eliminate organic contaminants and coliform bacteria from HWW.

### 3.2. EO process

Electrochemical technologies present a viable alternative for addressing various environmental challenges associated with wastewater treatment. This study used a Ti-TiO<sub>2</sub>/IrO<sub>2</sub>/RuO<sub>2</sub> anode mesh with a hollow cylindrical configuration to assess its performance in treating HWW. The effects of varying current densities were systematically analyzed to evaluate their impact on COD removal efficiency at regular time intervals [30]. The morphology and elemental composition of the pristine anode and cathode materials were examined via HR-SEM (Fig. 1). The anode surface exhibited a distinctive molded topology with pronounced surface cracking, which can be attributed to the thermal processing of the electrode fabrication at Ti substrate, subsequently coated with a layer of triple metal oxides (TiO<sub>2</sub>/IrO<sub>2</sub>/RuO<sub>2</sub>). The crack propagation range is from 5 to 20 μm, characterized by an initial broad width that narrows to a sharp edge (Fig. 1a) and (Fig. 1b), suggesting the influence of cavitation phenomena. This specific surface morphology is advantageous for chlorine evolution reactions, as supported by existing literature [30,31]. In addition, EDX analysis provided the atomic weight percentages of the constituents: titanium (Ti) at 67.60 %, ruthenium (Ru) at 30.80 %, and iridium (Ir) at 1.59 % supplementary information (Fig. S3a). These atomic weight percentages of the electrode correlate well with the thermal fabrication method utilized for the Ti plating with triple metal oxides. The stability of the TiO<sub>2</sub>, RuO<sub>2</sub>, and IrO<sub>2</sub> has been well established in EO applications [31]. The cathode displayed a flat surface profile, with emphasis on the presence of Ti (Fig. 1c&d). The prominent peak associated with the Ti element was uniquely observed in the EDX spectrum of the cathode supplementary information (Fig. S3 b).

This study examines the impact of applied current density on COD removal efficiency during the EO process of HWW using a Ti-TiO<sub>2</sub>/IrO<sub>2</sub>/RuO<sub>2</sub> mesh electrode system. The findings reveal a substantial correlation between variations in current density and the effectiveness of COD reduction throughout the EO treatment process. The COD removal efficiency exhibited a progressive increase over time across all tested current densities of 5.8, 10.4, and 15.5 mA/cm<sup>2</sup> (Fig. 2). Initially, there was a similar performance pattern across all current density configurations; however, significant variations in COD removal efficiencies

emerged by the end of the treatment period (Fig. 2). Remarkably, the system operating at 15.5 mA/cm<sup>2</sup> achieved the peak COD removal efficiency of 92 % after 10 h, while lower efficiencies of 42 % and 74 % were noted at 5.8 and 10.4 mA/cm<sup>2</sup>, respectively. Thus effectiveness of COD removal in HWW is substantially modulated by the specified current density, which is critical for the electrochemical generation of free active chlorine at the electrode interface [15]. In the undivided electrochemical cell arrangement, chlorine is generated at the hollow cylindrical Ti-TiO<sub>2</sub>/IrO<sub>2</sub>/RuO<sub>2</sub> mesh anode, while hydroxide ions (OH<sup>-</sup>) are generated at the Ti mesh cathode. The inter-electrode gap, maintained between 8 and 10 mm, is vital for facilitating the electrochemical reactions that yield chlorine and hypochlorite [11]. These reactions are influenced by the pH conditions of the HWW. The active chlorine species diffuse the flow of HWW, facilitating the oxidation of organic pollutants throughout the bulk solution [10–13]. This process contributes to demineralization, resulting in a significant decrease in COD levels. The reactions occurring in the portable electrochemical reactor during the EO process of HWW lead to a reduction in COD, as outlined in the proposed mechanistic framework [15,18,21,23].



The COD removal efficiency results indicate that the system operating at a current density of 15.5 mA/cm<sup>2</sup> outperforms other systems (Fig. 2). Consequently, this current density has been selected for subsequent analyses, including the assessment of physicochemical characterization, active chlorine production, total viable bacterial counts, morphology and crystal phase of electro deposition of cathode, distribution of heavy metals and the characterization of intermediate metabolites, which were examined using FT-IR and GC-MS.

**Table 2.** The comparative physicochemical analysis of raw and EO-treated HWW at a current density of 15.5 mA/cm<sup>2</sup>. The analysis focuses on key parameters with IS 10500: 2012 standards and the WHO guidelines for irrigation water quality [32]. The brown colour of raw HWW changed to a white hue, indicating a significant reduction in odour supporting information (Fig. S4). Notably, turbidity exhibited a two-fold decrease following EO treatment. Enhanced reduction performance was observed concerning TDS and TSS, with levels recorded at 760 ± 11.4 mg L<sup>-1</sup> and 380 ± 8.2 mg L<sup>-1</sup>, respectively. There was a substantial four-fold reduction in total hardness, 280 ± 8.2 mg l<sup>-1</sup>, and decreases in Ca and Mg levels, noted at 72 ± 2.5 mg L<sup>-1</sup> and 38 ± 2.2 mg L<sup>-1</sup>, respectively. In addition, the treatment resulted in notably reduced concentrations of NH<sub>3</sub> at 0.4 ± 0.0 mg L<sup>-1</sup>, NO<sub>3</sub> at 5.0 ± 0.2 mg L<sup>-1</sup>, and NO<sub>2</sub> at 0.09 ± 0.0 mg L<sup>-1</sup>. A four-fold decrease in BOD was recorded (180 ± 4.6 mg L<sup>-1</sup>) compared to that of raw HWW (Table .1). Fig. 3 depicts the temporal evolution of active chlorine species during the electrolysis process. Notably, there was a transient low concentration of active chlorine species observed between 30 and 60 min. However, the chlorine concentration exhibited a significant upward trend over time, culminating at a peak of 1240 ± 14.90 ppm (Fig. 3). This escalation in chlorine levels corresponded with a marked enhancement in COD removal efficiency (92 %), indicating a positive correlation between chlorine concentration and treatment efficacy. The physicochemical parameters indicate that this EO technology exhibits high efficiency in the treatment and safe disposal of HWW. Furthermore, an emerging area of research is the system's effectiveness in eradicating pathogens and viruses from hospital effluents, which highlights its potential role in infection control and environmental safety [10,14]. Supporting information (Table S1) presents the time required to determine the total viable bacterial counts for the EO time duration at a current

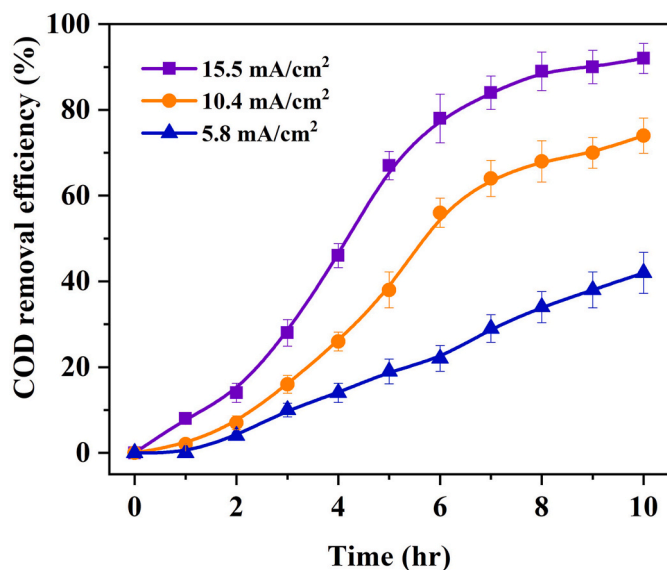
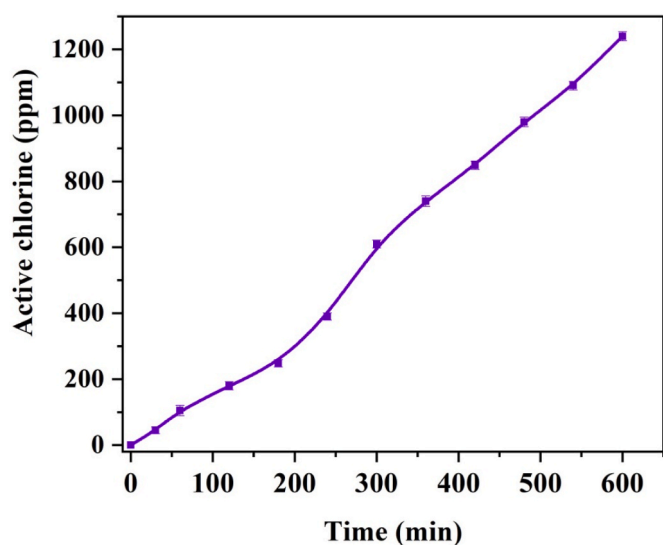


Fig. 2. Evaluation of the influence of varying current densities on the performance of the Ti-TiO<sub>2</sub>/IrO<sub>2</sub>/RuO<sub>2</sub> electrode and its corresponding COD removal efficiency.

**Table 2**

Comparative analysis of the GC-MS data concerning organic contaminants in both raw and EO-treated HWW.

S. No	Retention Time	Compound name	Raw	EO-treated HWW
1	8.47	Phenol, (m/z)94	+	+
2	10.48	Undecane, (m/z) 156	+	+
3	11.07	Dimethylsiloxane pentamer, (m/z)370	+	+
4	13.58	Cyclohexasiloxane, dodecamethyl-, (m/z) 444	+	+
5	15.80	Benzoic acid, 3-methyl-2-trimethylsilyloxy-, trimethylsilyl ester, (m/z) 296	+	+
6	17.76	2,5-Dihydroxybenzoic acid, 3TMS derivative, (m/z) 370	-	+
7	18.37	Tridecyl aldehyde, (m/z)198	+	-
8	18.46	1,2-Epoxytetradecane, (m/z) 212	+	-
9	18.88	Tetradecanoic acid, methyl ester, (m/z) 242	+	+
10	19.56	Stearic acid, methyl ester, (m/z)298	+	-
11	19.65	Cyclopentanetridecanoic acid, methyl ester, (m/z) 296	+	-
12	20.99	Undecanoic acid, 2-nonyl-, methyl ester, (m/z) 326	+	-
13	21.00	Methyl 2-nonylundecanoate, (m/z) 326	-	+
14	21.08	Benzene propanoic acid, 3,5-bis(1,1-dimethylethyl)-4-hydroxy-, methyl ester, (m/z) 292	+	+
15	22.63	9,12-Octadecadienoic acid, methyl ester, (m/z) 294	+	+
16	22.69	9-Octadecenoic acid (Z)-, methyl ester, (m/z) 296	+	+
17	22.92	Methyl stearate, (m/z) 298	+	+
18	26.07	Cholestanol, (m/z) 388	-	+
19	26.19	1,2-Benzenedicarboxylic acid, decyl octyl ester, (m/z) 418	+	+
20	26.20	Phthalic acid, butyl undecyl ester, (m/z) 376	-	+
21	26.45	Bis (2-ethylhexyl) 1,2-benzenedicarboxylate, (m/z) 390	-	+
22	27.68	Phenol, 2,4-bis(1,1-dimethylethyl)-, phosphite (3:1), (m/z) 646	+	+
23	28.25	13-Docosenamide, (Z)-, (m/z) 337	+	+
24	28.54	Di-3,7-dimethyl-1-octyl phthalate, (m/z) 446	+	+
25	29.43	Cholesteryl benzoate, (m/z) 490	-	+

**Fig. 3.** Measurement of active chlorine generation during the EO process at an applied current density of 15.5 mA/cm<sup>2</sup>.

density of 15.5 mA/cm<sup>2</sup>. The initial viable bacterial counts in the HWW were recorded at 8.4 x 10<sup>8</sup> CFU/ml. This elevation in bacterial prevalence is attributable to the diverse range of complex microbial ecosystems typical of healthcare waste, which is influenced by both patient-derived microorganisms and the presence of antimicrobial agents used in clinical treatments [1,33]. The EO process effectively eliminated bacterial species within 30 min, although a low-level enrichment of bacterial colonies was noted (S1). However, following a 60 min exposure, complete eradication of bacterial species was achieved (S1). Furthermore, an investigation into fecal coliforms and total coliforms, employing the MPN method, confirmed their absence, which can be ascribed to the active chlorine species generated electrochemically. These reactive species effectively compromised bacterial cell integrity within the wastewater matrix [34]. These findings emphasize the efficacy of the EO process in the removal of both pathogenic and non-pathogenic bacterial taxa from HWW, thus highlighting its substantial potential as an innovative solution for the management of healthcare-associated waste.

### 3.3. HR-SEM and XRD analysis of the scale deposition on the cathode

After EO-treatment of HWW, the cathode exhibited a white, slightly pale deposition. This material was subsequently analyzed for its morphological characteristics and crystal phase using HR-SEM and XRD techniques (Fig. 4a). illustrates the HR-SEM imaging of the cathode, revealing a fine micro flower-like slime layer that encompasses the cathode surface. An enlarged view of this layer highlights thread-like structures, with size distributions ranging from 0.6 to 1.5 μm (Fig. 4b). The edges of these threads display sharp, nano-needle-like features, and they aggregate to form a micro-flower structure. The nucleation process responsible for scale formation on the cathode surface was influenced by hardness-causing species such as Ca<sup>2+</sup> and Mg<sup>2+</sup> ions and HCO<sub>3</sub><sup>-</sup> [35,36]. During EO treatment, OH<sup>-</sup> ions generated at the cathode play a crucial role in determining the nucleation sites. These ions rapidly migrate into the bulk HWW and react with available Ca<sup>2+</sup> and Mg<sup>2+</sup> ions, thereby facilitating the growth of crystal nuclei on the electrode surface [36]. As crystal growth progressed, larger crystals eventually detached from the electrode due to the hydrogen evolution phenomena occurring at the cathode, along with gravitational sedimentation effects [37]. The EDX spectrum and elemental composition of the cathode are provided in (Fig. 4c) and supporting information (Table S2). The deposit composition was predominantly Mg (9.35 %) and Ca (0.86 %), with minimal amounts of P (0.41 %) and Fe (0.07 %). The XRD pattern proved the presence of calcite, magnesium calcite, and aragonite crystal phases in the materials deposited on the cathode (Fig. 5). These findings were supported by the physicochemical characterization of an HWW sample taken after EO treatment, which demonstrated a reduction in total hardness, and Ca and Mg contents (Table 1).

### 3.4. Distribution of heavy metals

Heavy metal contamination in wastewater discharge from industrial, domestic, and healthcare sources poses a significant challenge to effective treatment processes and is critical for protecting aquatic and soil ecosystems [38]. The presence of these contaminants can have detrimental effects on diverse biological communities. This study investigates the concentrations of heavy metals present in raw HWW and evaluates the reductions achieved through EO treatment, providing comparative insights into the effectiveness of this remediation technique [39]. Initial measurements indicated high concentrations of Fe, Cu, and Zn, recorded at 945 ± 14.0 ppm, 732 ± 12.0 ppm, and 650 ± 9.0 ppm, respectively. Mn and Pb were found at comparatively lower concentrations of 68 ± 3.0 ppm and 20 ± 1.0 ppm. Following EO treatment, substantial reductions in heavy metal concentrations were observed: Fe levels decreased to 450 ± 8.0 ppm, Cu to 345 ± 10.0 ppm, Zn to 140 ±

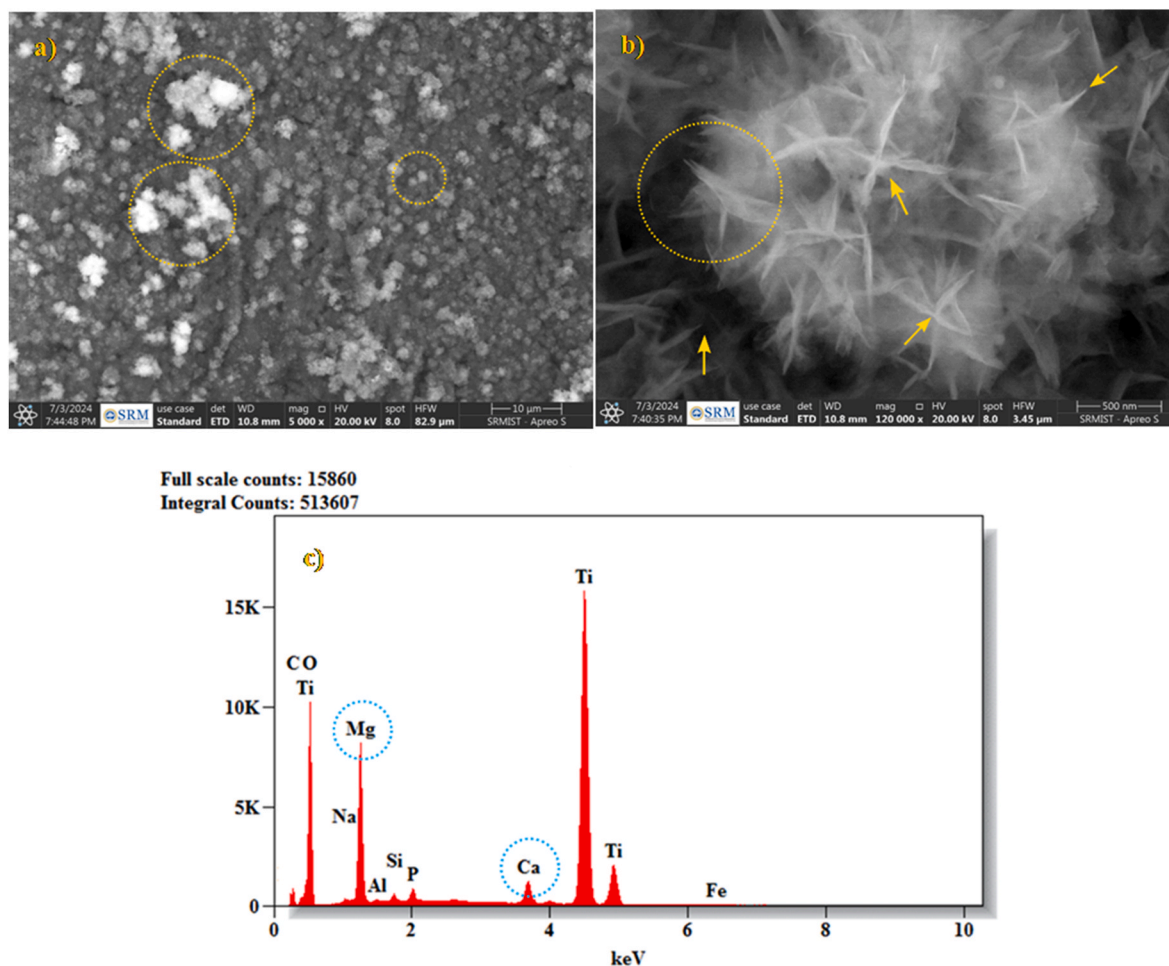


Fig. 4. (a & b) HR-SEM images and (c) EDX spectrum of the Ti electrode after 7 h of EO treatment of HWW.

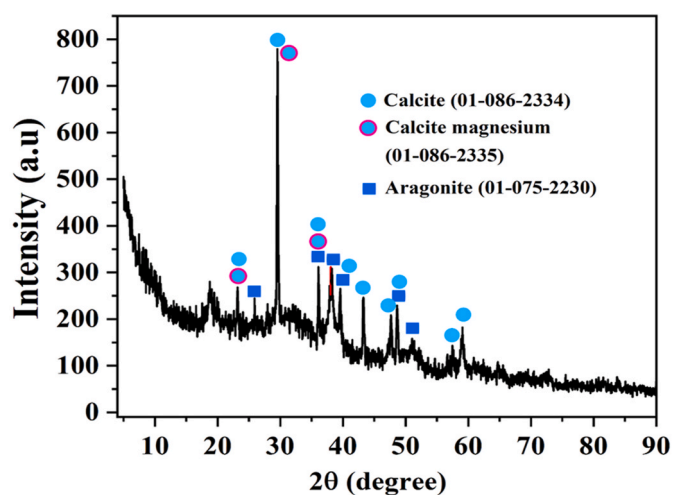


Fig. 5. XRD pattern of the precipitate formed on the Ti electrode surface after 7 h of EO treatment.

10.0 ppm, Mn to  $15.0 \pm 10.0$  ppm, and Pb to  $5.0 \pm 0.3$  ppm. The EO process operates through the generation of free chlorine, which facilitates the effective disruption of organic complexes associated with heavy metals in HWW [21]. This disruption may facilitate the transfer of heavy metals to the cathode surface, where interactions occur with Ca and Mg oxide layers. These interactions may result in the entrapment or

overlapping of deposited metals, thereby enhancing the removal efficiency of heavy metals from wastewater [21,36].

### 3.5. FT-IR and GC-MS study

A comparative analysis of the FT-IR spectra obtained before and after a 7 h EO treatment of HWW, performed at a current density of  $15.5 \text{ mA/cm}^2$ , reveals significant changes indicative of the electrochemical degradation of organic pollutants and the formation of intermediate organic metabolites (Fig. 6). The presence of distinct FT-IR peaks highlights the alterations in various organic functional groups. The FT-IR spectra of the HWW sample displayed a prominent band at  $3457 \text{ cm}^{-1}$ , indicating the presence of hydroxyl ( $\text{OH}^-$ ) functional groups. A less intense band at  $2937 \text{ cm}^{-1}$  corresponds to the symmetric and antisymmetric stretching vibrations of  $\text{CH}_2$  and  $\text{CH}_3$  groups. The peak at  $1647 \text{ cm}^{-1}$  is associated with the stretching vibration of the carbonyl ( $\text{C}=\text{O}$ ) group found in amide functional groups (Fig. 6). This suggests the presence of biomolecules such as urea and proteins, likely derived from urine or microbial activity, as well as various pharmaceutical compounds [40]. Additionally, the FT-IR band at  $1379 \text{ cm}^{-1}$  reflects the symmetric bending vibrations of  $\text{CH}_3$ , which highlight the presence of methyl groups typical of pharmaceutical substances. The peak at  $1109 \text{ cm}^{-1}$  corresponds to asymmetric stretching vibrations related to C–O bonds, which are relevant to urine and hardwater components in wastewater [41]. Furthermore, the FT-IR band at  $998 \text{ cm}^{-1}$  indicates C=O stretching vibrations, and it is related to organic pollutants [41]. Finally, the peak at  $618 \text{ cm}^{-1}$  can be attributed to metal-carboxylate functional groups. The FT-IR analysis of EO-treated HWW revealed significant

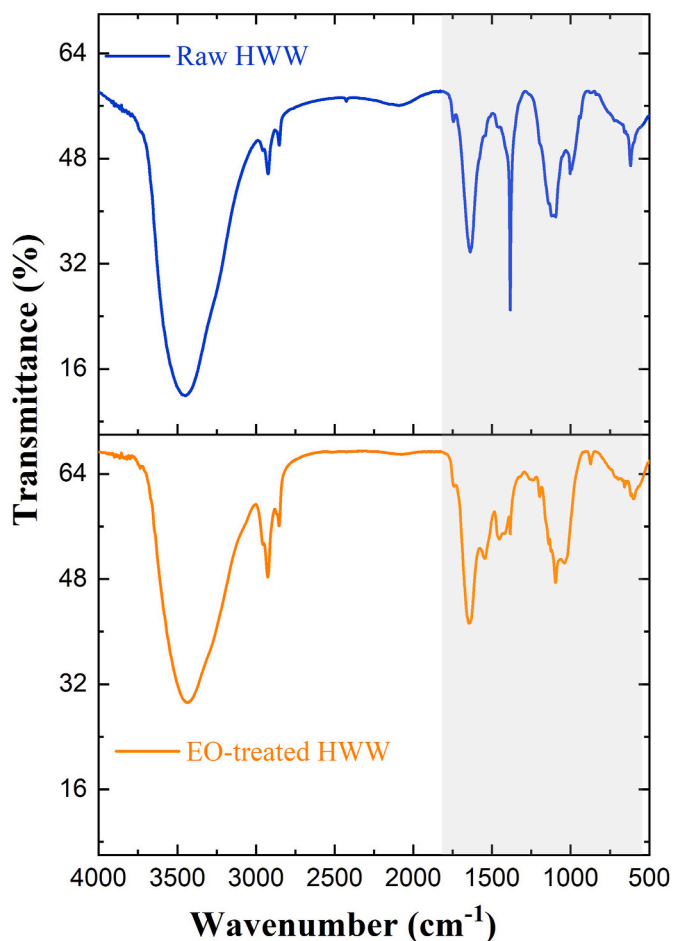


Fig. 6. FT-IR spectra comparison between raw HWW and EO-treated HWW.

spectral modifications, particularly bands at  $1545\text{ cm}^{-1}$  and  $1091\text{ cm}^{-1}$ , which are characteristic of amide-II and carbonyl functional groups, respectively. Additionally, a notable reduction was observed in the FT-IR peak at  $1397\text{ cm}^{-1}$ , along with diminished intensities in other spectral peaks (Fig. 6). These changes can be attributed to the indirect electrochemical generation of active chlorine, which initiates various oxidative reactions targeting organic constituents within the wastewater [12,16]. Overall, the FT-IR data indicate that EO treatment effectively leads to the degradation and removal of multiple organic functional groups from the HWW.

GC-MS analysis was employed to assess the alterations in the organic constituents of HWW before and after treatment with the Ti-TiO<sub>2</sub>/IrO<sub>2</sub>/RuO<sub>2</sub> anode electrocatalytic system, operated at a current density of  $15.5\text{ mA/cm}^2$ , as supporting information in (Fig. S5). (Table 2) summarizes the organic compounds identified in both raw and electrochemically oxidized HWW. The primary constituents of raw HWW included Methyl stearate ( $m/z$  298), Stearic acid methyl ester ( $m/z$  298), Undecanoic acid, 2-nonyl-, methyl ester ( $m/z$  326), (Z)-13-Docosenamide ( $m/z$  337), Di-3,7-dimethyl-1-octyl phthalate ( $m/z$  446), and Cholesteryl benzoate ( $m/z$  490). Methyl stearate and stearic acid methyl ester function as non-ionic surfactants, thereby enhancing the solubility of various compounds by disrupting aggregates and facilitating protein unfolding [42]. Docosenamide is noteworthy for its potential applications as an antimicrobial agent, anticancer compound, and bioactive fluid regulator [43]. Cholesteryl benzoate finds use in hair coloring and various household products. Additional lower intensity of organic constituents include Phenol ( $m/z$  94), Benzene propanoic acid, 3,5-bis(1,1-dimethylethyl)-4-hydroxy-, methyl ester ( $m/z$  292), a 2,5-Dihydroxybenzoic acid derivative ( $m/z$  370), 1,2-Benzene dicarboxylic acid, decyl

octyl ester ( $m/z$  418), Di-3,7-dimethyl-1-octyl phthalate ( $m/z$  446), and Phenol, 2,4-bis(1,1-dimethylethyl)-, and phosphite (3:1) ( $m/z$  646). The presence of phenolic compounds is significant due to their roles as disinfectants and antiseptics, while benzene propanoic acid serves as a food preservative and is utilized in pharmaceutical formulations [44]. The GC-MS analysis revealed the presence of key compounds such as phenols, esters, non-ionic surfactants, and amides, which are relevant to the chemical agents employed in hospitals and healthcare facilities. Nonetheless, there is a lack of evidence indicating the commercial use of pharmaceuticals or other drug formulations within HWW. The GC-MS chromatogram demonstrated a noticeable decrease in the overall intensity of organic compounds following EO treatment, indicating a reduction in the organic contents of the raw HWW sample (Table 2). Besides, various organic compounds have been subjected to investigation through oxidation processes facilitated by active chlorine production in an electrochemical reactor. This approach encompasses multiple oxidation stages, significantly contributing to the demineralization process of wastewater [30]. Furthermore, the GC-MS spectra revealed the absence of certain organic moiety peaks (Tridecyl aldehyde, ( $m/z$ ) 198, 1,2-Epoxytetradecane, ( $m/z$ ) 212 and cholesteryl benzoate, ( $m/z$ ) 490) and accompanied by the appearance of new peaks (2,5-Dihydroxybenzoic acid, 3 TMS derivative, ( $m/z$ ) 370 and Cholestanol, ( $m/z$ ) 388), which points to significant alterations in the organic compound profile throughout the treatment process (Table 2). Further studies are necessary on electrochemically treated HWW to evaluate its toxicity assessments using seed germination assays and plant growth parameters. These studies could provide valuable insights for evaluating the suitability of treated HWW for irrigation purposes and its implications for the integrity of soil ecosystems.

### 3.6. XRD pattern of before and after EO-treated HWW

This research investigates the reusability and material stability of the Ti-TiO<sub>2</sub>/IrO<sub>2</sub>/RuO<sub>2</sub> mesh electrode across four consecutive operational cycles, with an emphasis on its electrochemical performance as assessed by the levels of COD removal rates (Fig. 7a). The electrochemical treatment of HWW was executed at a current density of  $15.5\text{ mA/cm}^2$  under optimized conditions, achieving a COD removal efficiency of 92 % over after 10 h during the initial three cycles. Notably, a slight decline in COD removal efficiency to 91 % was recorded in the fourth cycle, indicating minor degradation in electrode performance. Material stability was evaluated using XRD analysis, revealing no significant alterations in the crystal phases of the electrode (TiO<sub>2</sub>, RuO<sub>2</sub>, and IrO<sub>2</sub>) after four treatment cycles, thereby affirming its material integrity (Fig. 7b). Moreover, the findings suggest that effective COD at moderate pH levels and lower current densities is beneficial for sustaining EO performance during wastewater treatment. Previous studies have emphasized the synergistic effects of TiO<sub>2</sub>, RuO<sub>2</sub>, and IrO<sub>2</sub> on the Ti substrate, which enhanced electro stability and durability during chlorine evolution reactions [16,18]. The Ti substrates, comprised of a triple metal oxide with diverse electrode configurations, show promise for applications within the chlor-alkali sector, as well as for both industrial and domestic wastewater treatment.

### 3.7. Toxicity assessments

The toxicity values are systematically presented in the supplementary information (Table S3). The analysis indicated a notable reduction in the toxicity levels of the majority of compounds present in HWW following the EO treatment. GC-MS data highlighted a significant decrease in ester derivatives within the HWW after EO treatment, correlating with lowered toxicity levels in the effluent (Table 2). Specifically, the elevated acute toxicity (LC50, EC50) and ChV for compounds such as phenol 2,4-bis(1,1-dimethylethyl)-phosphite were substantially mitigated by the EO process. The ECOSAR tool utilizes theoretical and computational models to assess the water solubility

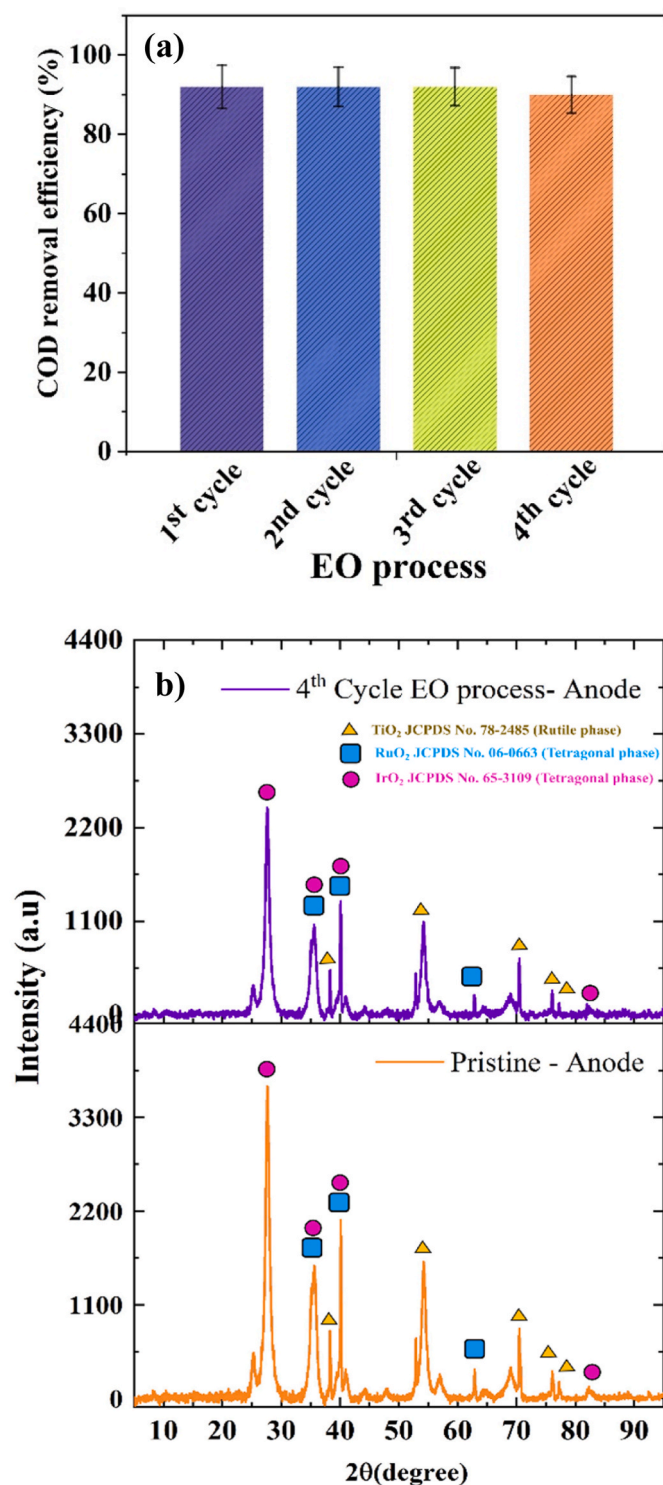


Fig. 7. a) Recycle performance of COD removal by Ti–TiO<sub>2</sub>/IrO<sub>2</sub>/RuO<sub>2</sub> mesh electrode, b) XRD pattern of before and after EO- treated HWW.

parameters of various compounds, thereby enhancing toxicity evaluations. Nonetheless, the toxicity profile of HWW is complicated by the diverse interplay between water-insoluble and soluble surfactants and organic compounds, as well as their interactions with other contaminants, including heavy metals [2,3]. The characteristics of EO intermediate products also exhibit variability compared to their parent compounds. Consequently, future research focuses on an in-depth analysis of fish toxicity levels in both raw HWW and EO-treated

effluent to elucidate the underlying mechanisms of toxicity and improve assessments.

(Table S4) Supplementary information provides a comparative analysis of the EO performance of the hollow cylindrical anode relative to other Ti-substrate electrodes coated with metal oxides used in HWW treatment. This study focuses on the use of a hollow cylindrical Ti–TiO<sub>2</sub>/IrO<sub>2</sub>/RuO<sub>2</sub> mesh electrode for the treatment of HWW. The mesh design enhances the electroactive catalytic surface area, which facilitates better interaction with Cl<sup>-</sup> ions present in HWW, thus improving the production of active chlorine species [45]. The experimental setup includes a portable continuous flow reactor that promotes efficient mass transfer during electrochemical reactions, leading to a notable increase in potential oxidants that can react with the bulk HWW. This configuration is advantageous for scaling up treatment capacity without the need to revamp the entire system. The past research explored the electrochemical degradation mechanisms of individual antibiotics as well as their mixtures in HWW, offering critical insights for the optimization of EO parameters [10–13]. It was found that employing optimal concentrations of NaCl in the treatment of wastewater significantly enhances the electro-oxidative degradation of organic contaminants, facilitated by an indirect chlorine-mediated process [13]. Characterization of the HWW revealed Cl<sup>-</sup> ions concentrations of  $1800 \pm 16.0 \text{ mg L}^{-1}$ , which were effectively leveraged to generate active chlorine at the mesh anode (Ti–TiO<sub>2</sub>/IrO<sub>2</sub>/RuO<sub>2</sub>) during the electrolysis process. This generated active chlorine is pivotal for the hetero-oxidation of organic pollutants, leading to significantly improved COD removal rates (92%). Additionally, the FT-IR and GC-MS analyses reveal that the oxidation of organic pollutants occurs in multiple stages, significantly enhancing the demineralization process of the wastewater (Table .2). This process also potentially assists in the removal of heavy metals bound within the organic matrix. The total hardness observed in the HWW was significantly elevated ( $1400 \pm 12.5 \text{ mg L}^{-1}$ ), and the application of EO treatment resulted in a marked reduction in total hardness levels ( $280 \pm 4.8 \text{ mg L}^{-1}$ ). This reduction is likely attributable to the precipitation of hardness-related constituents (calcite, magnesium calcite, and aragonite) at the cathode [36]. In addition, this process could facilitate the entrapment of heavy metals within these precipitated forms. Chlorine is well-recognized for its efficacy as a disinfectant in the treatment of drinking water [34]. Recent advancements in electro chlorination technologies have gained prominence due to their capacity to effectively inactivate pathogenic microorganisms in HWW [46]. This is achieved through oxidative mechanisms that disrupt the structural integrity of pathogen cell walls, leading to rapid inactivation [47].

Furthermore, the treatment effectively eliminated total coliforms, fecal coliforms, and other microbial contaminants within 1 h of the EO process supporting information (Table S1). The physicochemical parameters of the EO-treated HWW were significantly below the discharge thresholds outlined in IS 10500: 2012, as well as the WHO guidelines for irrigation water quality [32]. The implementation of hollow cylindrical mesh electrodes in portable electrochemical reactors offers a viable and advanced approach in addressing the issues associated with the intricate residues of pharmaceuticals and chemical reagents, as well as the presence of pathogenic microorganisms in hospital effluents. This portable electrochemical reactor design with Ti–TiO<sub>2</sub>/IrO<sub>2</sub>/RuO<sub>2</sub> mesh electrode enhances the efficiency of electrochemical processes and enables more effective degradation and removal of contaminants, making it an effective solution for treating HWW.

### 3.8. Operational expenses

This investigation assesses the economic viability of a portable electrochemical reactor designed for HWW treatment. The reactor can be constructed using cost-effective materials, predominantly standard glass, accompanied by a mini water pump and silicone tubing, resulting in an economical design. The estimated costs for Ti–TiO<sub>2</sub>/IrO<sub>2</sub>/RuO<sub>2</sub> and Ti mesh electrode were 14.01 and 9.34 USD, respectively. These

electrodes are renowned for their robust durability and high efficiency in EO processes [18]. The energy consumption associated with the EO treatment is directly influenced by the concentration of organic pollutants present in the wastewater. Preliminary estimates indicate that the cost of treating 1000 L of HWW using the EO method with the Ti-TiO<sub>2</sub>/IrO<sub>2</sub>/RuO<sub>2</sub> mesh electrode is approximately USD 30.10. Notably, the cost of electrodes significantly dominated electricity consumption in the overall expense of the electrochemical reactor fabrication for EO treatment. Furthermore, this study provides a comprehensive cost analysis aimed at incorporating these portable reactors into cluster-level wastewater treatment systems. The proposal also includes pilot-scale deployments at hospitals and healthcare facilities, facilitating the generation of discharge-quality effluent suitable for irrigation applications.

#### 4. Conclusion

The pilot-scale implementation of the EO process has effectively tackled critical challenges in treating HWW, achieving significant reductions in COD, BOD, and total hardness through the utilization of a Ti-TiO<sub>2</sub>/IrO<sub>2</sub>/RuO<sub>2</sub> mesh anode. The study investigated various current densities (5.8, 10.4, and 15.5 mA/cm<sup>2</sup>), resulting in COD removal efficiencies of 42 %, 74 %, and 92 %, respectively. This substantial decrease in COD can be attributed to the enhanced generation of active chlorine species, which peaked at 1240 ± 14.0 ppm during the EO process. Importantly, fecal, total coliforms and various bacterial populations were effectively eradicated within a 60-min treatment. FT-IR and GC-MS analyses confirmed that electro chlorination significantly facilitated the breakdown of organic pollutants in HWW, leading to the formation of several intermediate organic metabolites. A four-fold reduction in total hardness was accomplished through the integration of a hollow cylindrical titanium mesh cathode during the EO process. HR-SEM and XRD analyses evidenced the formation of a slime layer on the electrode surface, alongside the development of micro-flower clusters comprising calcite, magnesium calcite, and aragonite crystal phases. Additionally, AAS provided conclusive proof of effective heavy metal removal from industrial wastewater utilizing the EO method. The durability and reusability of the Ti-TiO<sub>2</sub>/IrO<sub>2</sub>/RuO<sub>2</sub> mesh electrode were confirmed across four consecutive operational cycles, underscoring the robust performance of both the EO process and the electrode material. These findings underscore the reliability and efficacy of the pilot-scale electrochemical reactor as a promising technology for treating hazardous wastewater, ultimately enhancing water quality for agricultural irrigation.

#### CRedit authorship contribution statement

**Vinoth kumar Palur Manoharan:** Writing – review & editing, Writing – original draft, Software, Methodology, Data curation, Conceptualization. **Perumal Dhandapani:** Visualization, Validation, Methodology, Investigation, Data curation. **Madhan Kumar Pichandi:** Validation, Software, Data curation, Visualization, Writing – original draft, Writing – review & editing. **Aruliah Rajasekar:** Validation, Software. **Punniyakotti Parthipan:** Validation. **Rajyoganandh Subramanian Vijayarman:** Writing – review & editing. **S.M. Prasad:** Validation. **Sudharsan Kasirajan:** Writing – review & editing, Visualization, Validation, Supervision, Software, Resources, Project administration, Methodology, Investigation, Formal analysis, Data curation, Conceptualization.

#### Informed consent statement

Not applicable.

#### Institutional statement review board

Not applicable.

#### Declaration of competing statement

The authors declare that they have no known competing financial interests or personal relationships that could have appeared to influence the work reported in this paper.

#### Appendix A. Supplementary data

Supplementary data to this article can be found online at <https://doi.org/10.1016/j.jics.2025.101985>.

#### Data availability

The data that has been used is confidential.

#### References

- [1] T.S. Oliveira, Environmental contamination from health-care facilities, *J. Health Pollut.* (2018) 7–19, <https://doi.org/10.1016/B978-0-444-63857-1.00002-4>.
- [2] B.S. Akin, Contaminant properties of hospital clinical laboratory wastewater: a physicochemical and microbiological assessment, *J. Environ. Protect.* 7 (5) (2016) 635, <https://doi.org/10.4236/jep.2016.75057>.
- [3] E. Emmanuel, Y. Perrodin, G. Keck, J.M. Blanchard, P. Vermande, Ecotoxicological risk assessment of hospital wastewater: a proposed framework for raw effluents discharging into urban sewer network, *J. Hazard. Mater.* 117 (1) (2005) 1–11, <https://doi.org/10.1016/j.jhazmat.2004.08.032>.
- [4] A.K. Gautam, S. Kumar, P.C. Sabumon, Preliminary study of physico-chemical treatment options for hospital wastewater, *J. Environ. Manag.* 83 (3) (2007) 298–306, <https://doi.org/10.1016/j.jenvman.2006.03.009>.
- [5] B. Tiwari, B. Sellamuthu, Y. Ouarda, P. Drogui, R.D. Tyagi, G. Buelna, Review on fate and mechanism of removal of pharmaceutical pollutants from wastewater using biological approach, *Bioresour. Technol.* 224 (2017) 1–12, <https://doi.org/10.1016/j.biortech.2016.11.042>.
- [6] A. Kumari, N.S. Maurya, B. Tiwari, Hospital wastewater treatment scenario around the globe, *Curr. Dev. Biotechnol. Bioeng.* (2020) 549–570, <https://doi.org/10.1016/B978-0-12-819722-6.00015-8>. Elsevier.
- [7] M. Dolatabadi, S. Ahmadzadeh, Catalytic ozonation process using modified activated carbon as a catalyst for the removal of sarafloxacin antibiotic from aqueous solutions, *Anal. Methods Environ. Chem.* 6 (2) (2023) 31–41.
- [8] Z. Liu, S. Hosseinzadeh, N. Wardenier, Y. Verheust, M. Chys, S.V. Hulle, Combining ozone with UV and H<sub>2</sub>O<sub>2</sub> for the degradation of micropollutants from different origins: lab-scale analysis and optimization, *Environ. Technol.* 40 (28) (2019) 3773–3782, <https://doi.org/10.1080/09593330.2018.1491630>.
- [9] A. Gallo-Cordova, J.J. Castro, E.L. Winkler, E. Lima Jr., R.D. Zysler, M. del Puerto Morales, J.G. Ovejero, D.A. Streitwieser, Improving degradation of real wastewaters with self-heating magnetic nanocatalysts, *J. Clean. Prod.* 308 (2021) 127385, <https://doi.org/10.1016/j.jclepro.2021.127385>.
- [10] G. Bhandari, P. Chaudhary, S. Gangola, S. Gupta, A. Gupta, M. Rafatullah, A review on hospital wastewater treatment technologies: current management practices and future prospects, *J. Water Process Eng.* 56 (2023) 104516, <https://doi.org/10.1016/j.jwpe.2023.104516>.
- [11] A.H. Khan, N.A. Khan, S. Ahmed, A. Dhingra, C.P. Singh, S.U. Khan, A. Mohammadi, F. Changani, M. Yousefi, S. Alam, S. Vambol, Application of advanced oxidation processes followed by different treatment technologies for hospital wastewater treatment, *J. Clean. Prod.* 269 (2020) 122411, <https://doi.org/10.1016/j.jclepro.2020.122411>.
- [12] S.W. da Silva, J.B. Welter, L.L. Albornoz, A.N.A. Heberle, J.Z. Ferreira, A. M. Bernardes, Advanced electrochemical oxidation processes in the treatment of pharmaceutical containing water and wastewater: a review, *Curr. Pollut. Rep.* 7 (2021) 146–159, <https://doi.org/10.1007/s40726-021-00176-6>.
- [13] J. Liu, N. Ren, C. Qu, S. Lu, Y. Xiang, D. Liang, Recent advances in the reactor design for industrial wastewater treatment by electro-oxidation process, *Water* 14 (22) (2022) 3711, <https://doi.org/10.3390/w14223711>.
- [14] M. Dolatabadi, M.H. Ehrampoush, M. Pournamdari, A.A. Ebrahimi, H. Fallahzadeh, S. Ahmadzadeh, Catalytic electrodes' characterization study serving polluted water treatment: environmental healthcare and ecological risk assessment, *J. Environ. Sci. Health, Part B* 58 (9) (2023) 594–602.
- [15] W. Hu, D. Yang, Y. Chang, K. Yu, L. Yang, W. Yan, H. Xu, X. Wu, Electrocatalytic oxidation for organic wastewater: recent progress in anode material, reactor, and process combination, *Chem. Eng. J.* (2024) 154120, <https://doi.org/10.1016/j.cej.2024.154120>.
- [16] R.S. de Santana Castro, A.R. Doria, M.B. Ferreira, K.I.B. Eguluz, G.R. Salazar-Banda, Advancements in mixed metal oxide anodes for efficient electrochemical treatment of wastewater, *Adv. Chem. Pollut. Environ. Manag. Protect.* 10 (2024) 191–218, <https://doi.org/10.1016/bs.apmp.2023.07.001>.

- [17] P. Iovino, S. Chianese, A. Fenti, J. Blotvogel, D. Musmarra, An innovative approach for atrazine electrochemical oxidation modelling: process parameter effect, intermediate formation and kinetic constant assessment, *Chem. Eng. J.* 474 (2023) 146022, <https://doi.org/10.1016/j.cej.2023.146022>.
- [18] Z. Yi, C. Kangning, W. Wei, J. Wang, S. Lee, Effect of IrO<sub>2</sub> loading on RuO<sub>2</sub>-IrO<sub>2</sub>-TiO<sub>2</sub> anodes: a study of microstructure and working life for the chlorine evolution reaction, *Ceram. Int.* 33 (6) (2007) 1087–1091, <https://doi.org/10.1016/j.ceramint.2006.03.025>.
- [19] P. Aravind, V. Subramanyan, S. Ferro, R. Gopalakrishnan, Eco-friendly and facile integrated biological-cum-photo assisted electrooxidation process for degradation of textile wastewater, *Water Res.* 93 (2016) 230–241, <https://doi.org/10.1016/j.watres.2016.02.041>.
- [20] P. Aravind, H. Selvaraj, S. Ferro, M. Sundaram, An integrated (electro-and bio-oxidation) approach for remediation of industrial wastewater containing azo-dyes: understanding the degradation mechanism and toxicity assessment, *J. Hazard. Mater.* 318 (2016) 203–215, <https://doi.org/10.1016/j.jhazmat.2016.07.028>.
- [21] P. Dhandapani, V. Srinivasan, P. Parthipan, M.S. AlSalhi, S. Devanesan, J. Narenkumar, R. Rajamohan, V. Ezhilselvi, A. Rajasekar, Development of an environmentally sustainable technique to minimize the sludge production in the textile effluent sector through an electrokinetic (EK) coupled with electrooxidation (EO) approach, *Environ. Geochem. Health* 46 (3) (2024) 81, <https://doi.org/10.1007/s10653-023-01847-7>.
- [22] R. Duraimurugan, P. Dhandapani, P. Velu, P. Parthipan, S. Devanesan, M. S. AlSalhi, A. Rajasekar, R. Babujanathanam, Sequential approach of photoelectrochemical oxidation and biodegradation of reverse osmosis reject water from the tannery industry, *J. Environ. Chem. Eng.* 13 (1) (2025) 115078, <https://doi.org/10.1016/j.jece.2024.115078>.
- [23] R.B. Baird, A.D. Eaton, E.W. Rice, L.S. Clesceri (Eds.), *Standard Methods for the Examination of Water and Wastewater*, 23rd edition, American Public Health Association (APHA), American Water Works Association (AWWA) and Water Environment Federation (WEF), Washington D.C., USA, 2017.
- [24] S. Rubini, G. Galletti, E. Bolognesi, P. Bonilauri, M. Tamba, F. Savini, A. Serraino, F. Giacometti, Comparative evaluation of Most probable number and direct plating methods for enumeration of *Escherichia coli* in *Ruditapes philippinarum*, and effect on classification of production and relaying areas for live bivalve molluscs, *Food Control* 154 (2023) 110005.
- [25] S. Kasirajan, D. Umapathy, C. Chandrasekar, V. Aafrin, M. Jenitapeter, L. Udhyasooriyan, S. Muthusamy, Preparation of poly (lactic acid) from *Prosopis juliflora* and incorporation of chitosan for packaging applications, *JBB* 128 (3) (2019) 323–331, <https://doi.org/10.1016/j.jbbiosc.2019.02.013>.
- [26] K.R. Rakhavan, K. Sudharsan, S. Babuskin, M. Sukumar, Design and characterization of spice fused tamarind starch edible packaging films, *LWT* 68 (2016) 642–652, <https://doi.org/10.1016/j.lwt.2016.01.004>.
- [27] S. Babuskin, P.A.S. Babu, M. Sasikala, K. Sabina, G. Archana, M. Sivarajan, M. Sukumar, Antimicrobial and antioxidant effects of spice extracts on the shelf life extension of raw chicken meat, *Int. J. Food Microbiol.* 171 (2014) 32–40, <https://doi.org/10.1016/j.ijfoodmicro.2013.11.011>.
- [28] K. Sudharsan, C.C. Mohan, P.A.S. Babu, G. Archana, K. Sabina, M. Sivarajan, M. Sukumar, Production and characterization of cellulose reinforced starch (CRT) films, *Int. J. Biol. Macromol.* 83 (2016) 385395, <https://doi.org/10.1016/j.ijbiomac.2015.11.037>.
- [29] P.M. Kumar, R. Babujanathanam, R.T. Selvi, R. Ganesamoorthy, S.J.J. Sudan, K. Kasthuri, R. Parameswari, Spherical-shaped ZnO nanoparticles and their diverse surface morphological applications in various biological applications against ROS, *Applied Physics A* 131 (5) (2025) 379, <https://doi.org/10.1007/s00339-025-08504-z>.
- [30] F. Long, D. Ghani, R. Huang, C. Zhao, Versatile electrode materials applied in the electrochemical advanced oxidation processes for wastewater treatment: a systematic review, *Sep. Purif. Technol.* (2024) 128725, <https://www.mdpi.com/2227-9717/13/4/987>.
- [31] P. Murugesan, P. Aravind, N. Guruswamy Muniyandi, S. Kandasamy, Performance of three different anodes in electrochemical degradation of 4-para-nitrophenol, *Environ. Technol.* 36 (20) (2015) 2618–2627.
- [32] J. Hassoune, F.Z. Karmil, B. Benhniya, F. Lakhdar, S. Etahiri, Hospital wastewater treatment using electrocoagulation: performance, kinetics, settlement analysis, and cost-effectiveness, *Desalin. Water Treat.* 317 (2024) 100226, <https://doi.org/10.1016/j.dwt.2024.100226>.
- [33] T. Yuan, Y. Pian, Hospital wastewater as hotspots for pathogenic microorganisms spread into aquatic environment: a review, *Front. Environ. Sci.* 10 (2023) 1091734.
- [34] U.H.N.M. Jefri, A. Khan, Y.C. Lim, K.S. Lee, K.B. Liew, Y.W. Kassab, C.Y. Choo, Y. M. Al-Worafi, L.C. Ming, A. Kalusalingam, A systematic review on chlorine dioxide as a disinfectant, *J. Med. Life.* 15 (3) (2022) 313.
- [35] C. Zhang, J. Tang, G. Zhao, Y. Tang, J. Li, F. Li, Y. Zhang, Investigation on electrochemical pilot equipment for water softening with an automatic descaling system: parameter optimization and energy consumption analysis, *J. Clean. Prod.* 276 (2020) 123178, <https://doi.org/10.1016/j.jclepro.2020.123178>.
- [36] M. Santhanam, R. Selvaraj, M. Sundaram, A two-step electrochemical method for separating Mg (OH) 2 and CaCO<sub>3</sub>: application to RO reject and polluted groundwater, *Chemosphere* 358 (2024) 142212, <https://doi.org/10.1016/j.chemosphere.2024.142212>.
- [37] M. Piri, R. Arefinia, Investigation of the hydrogen evolution phenomenon on CaCO<sub>3</sub> precipitation in artificial seawater, *Desalination* 444 (2018) 142–150.
- [38] J. Briffa, E. Sinagra, R. Blundell, Heavy metal pollution in the environment and their toxicological effects on humans, *Heliyon* 6 (9) (2020) e04691.
- [39] N.A. Qasem, R.H. Mohammed, D.U. Lawal, Removal of heavy metal ions from wastewater: a comprehensive and critical review, *npj Clean Water* 4 (1) (2021) 1–15.
- [40] V. Kumari, A.K. Tripathi, Characterization of pharmaceuticals industrial effluent using GC-MS and FT-IR analyses and defining its toxicity, *Appl. Water Sci.* 9 (2019) 1–8.
- [41] S. Álvarez-Torrellas, J.A. Peres, V. Gil-Álvarez, G. Ovejero, J. García, Effective adsorption of non-biodegradable pharmaceuticals from hospital wastewater with different carbon materials, *Chem. Eng. J.* 320 (2017) 319–329.
- [42] P.Y. Chen, C.Y.C. Wu, G.A. Clemons, C.T. Citadin, A.C. e Silva, H.E. Possioit, R. Azizbayeva, N.E. Forren, C.H. Liu, K.S. Rao, D.M. Krzywanski, Stearic acid methyl ester affords neuroprotection and improves functional outcomes after cardiac arrest, *PLEFA* 159 (2020) 102138.
- [43] N. El-Gazzar, L. Said, F.O. Al-Otibi, M.R. AbdelGawwad, G. Rabie, Antimicrobial and cytotoxic activities of natural (Z)-13-docosenamide derived from *Penicillium chrysogenum*, *Front. Cell. Infect. Microbiol.* 15 (2025) 1529104.
- [44] A. Del Olmo, J. Calzada, M. Nuñez, Benzoic acid and its derivatives as naturally occurring compounds in foods and as additives: uses, exposure, and controversy, *Crit. Rev. Food Sci. Nutr.* 57 (14) (2017) 3084–3103.
- [45] C. Wei, S. Sun, D. Mandler, X. Wang, S.Z. Qiao, Z.J. Xu, Approaches for measuring the surface areas of metal oxide electrocatalysts for determining their intrinsic electrocatalytic activity, *Chem. Soc. Rev.* 48 (9) (2019) 2518–2534.
- [46] C.A. Martínez-Huitle, M. Panizza, Electrochemical oxidation of organic pollutants for wastewater treatment, *Curr Opin Electroche* 11 (2018) 62–71.
- [47] H.T. Nguyen, W. Choi, S. Jeong, H. Bae, S. Oh, K. Cho, Comprehensive assessment of chlorination disinfection on microplastic-associated biofilms, *J. Hazard. Mater.* 474 (2024) 134751.